Anat Sci Int (2016) 91:8–21
DOI 10.1007/s12565-015-0303-0

REVIEW ARTICLE

Molecular and anatomical evidence for the input pathway- and target cell type-dependent regulation of glutamatergic synapses

Miwako Yamasaki[1]

Received: 14 August 2015 / Accepted: 17 September 2015 / Published online: 6 October 2015

Abstract Glutamate mediates most fast excitatory transmission in the central nervous system by activating primarily two types of ionotropic glutamate receptors: α-amino-3-hydroxy-5-methyl-4-isoxazole propionic acid (AMPA) and *N*-methyl-D-aspartate (NMDA) receptors. Differential subunit combinations generate great functional diversity in both categories of receptors, making them highly suitable for meeting complex functional requirements. Converging evidence has indicated that distinct AMPA and NMDA receptor subtypes are selectively targeted to functionally different synapses according to different factors, including presynaptic inputs, postsynaptic cell types, and synaptic configurations. This article provides an overview of recent progress in understanding the basic principles governing the synaptic allocation of AMPA and NMDA receptors, and discusses the underlying mechanisms and functional implications.

Keywords Glutamate receptor · AMPA receptor · NMDA receptor · Hippocampus · Purkinje cell · Interneuron · Immunohistochemistry · Mouse

Introduction

Glutamate mediates most of the fast excitatory transmission in the brain by activating primarily two types of ionotropic glutamate receptors: α-amino-3-hydroxy-5-methyl-4-isoxazole propionic acid (AMPA) and *N*-methyl-D-aspartate (NMDA) receptors. Whereas AMPA receptors (AMPARs) depolarize the postsynaptic neuron to set off firing, NMDA receptors (NMDARs) cause a large influx of calcium, which induces synaptic plasticity (Cull-Candy et al. 2001; Huganir and Nicoll 2013). Several subunits have been distinguished in each subfamily, and different subunit combination generates great diversity in biophysical properties, making them highly suitable for meeting complex functional requirements (Isaac et al. 2007; Kullmann and Lamsa 2007). In the neural circuit, these receptors are differentially allocated to synapses according to various factors, including presynaptic inputs, target cell types, and synaptic configurations, thereby extending the computational properties of neurons (Toth and McBain 1998; Brunel et al. 2004; Nicholson et al. 2006). In this review, I first provide a short overview of the morphological techniques required for analyzing the cellular and subcellular distributions of ionotropic glutamate receptors, and then discuss the cell type- and input-pathway-dependent allocations of synaptic glutamate receptors, focusing mainly on our recent work.

Technical considerations

Single-cell RT-PCR and isotopic in situ hybridization (ISH) studies have provided useful information about the expression patterns of ionotropic glutamate receptor subunits. ISH has been one of the most powerful methods available to examine the spatiotemporal pattern of gene expression. Although the original methods for ISH using radiolabeled probes are highly effective in detecting very low levels of transcripts (John et al. 1969), their major limitations are relatively poor cellular resolution and long exposure time. The more recently developed fluorescence

✉ Miwako Yamasaki
k-minobe@med.hokudai.ac.jp

[1] Department of Anatomy, Hokkaido University Graduate School of Medicine, Sapporo 060-8638, Japan

ISH (FISH) protocol, using tyramide signal amplification (TSA), has overcome these limitations and proven to be efficient and useful. It allows for the detection of virtually any combination of two or three mRNAs and for histochemical labeling in combination with immunofluorescence and tracer labeling, on the same sections. This facilitates the neurochemical identification of cellular and neuronal populations expressing the mRNA of interest.

However, simply knowing the mRNA expression level of receptors is not sufficient for making functional predictions, because neurons bear elaborated dendritic arbors to receive synaptic inputs from multiple sources, and receptors are not distributed evenly on the cell surface. Thus, the precise subcellular distribution pattern, including the density in each subcellular compartment and relationship with various synaptic inputs, must be determined. In clear contrast to intracellular and extrasynaptic receptors, synaptic AMPARs and NMDARs are concentrated at the postsynaptic density (PSD), and are not detected readily by conventional immunofluorescence and preembedding immunoelectron microscopy (Fritschy et al. 1998; Watanabe et al. 1998; Fukaya and Watanabe 2000). Therefore, detection of synaptic AMPARs and NMDARs requires antigen-unmasking procedures including protease (e.g., pepsin) pretreatment or postembedding immunogold electron microscopy (EM), both of which have been proven to yield compatible results (Ottersen and Landsend 1997; Fukaya and Watanabe 2000; Fukaya et al. 2006). Of the methods used currently, postembedding immunogold EM seems to be the most reliable and convenient for localizing and quantifying postsynaptic ionotropic neurotransmitter receptors (Ottersen and Landsend 1997; Petralia and Wenthold 1999). In postembedding immunogold EM, immunolabeling takes place on the very surface of ultrathin sections where antigens are easily accessible, allowing the high-resolution localization and quantification of receptors. Double labeling with appropriate marker proteins is quite efficient in determining the neurochemical identity of pre- and post-synaptic elements, making it possible to investigate the basic principles governing the subcellular distribution of ionotropic glutamate receptors.

Target cell type- and input pathway-dependent regulation of AMPAR expression

Qualitative difference in AMPAR expression

AMPARs are hetero- or homo-tetramers derived from subunits GluA1–4 (GluR1–4; GluRA–D) (Borges and Dingledine 1998; Collingridge et al. 2009). The subunit composition of AMPARs greatly influences the mode of synapse trafficking as well as their biophysical properties (Malinow and Malenka 2002; Bredt and Nicoll 2003; Huganir and Nicoll 2013). AMPARs that lack GluA2 are permeable to Ca^{2+} ions, exhibit a high single-channel conductance and display an inwardly rectifying I–V relationship as they are blocked by endogenous intracellular polyamines at positive potentials (Bowie and Mayer 1995; Koh et al. 1995a). The majority of AMPARs in the central nervous system (CNS) are GluA2-containing AMPARs (Wenthold et al. 1996; Greger et al. 2002). In the forebrain, GluA1 and GluA2 are the predominant subunits, with low levels of GluA3 and GluA4 (Monyer et al. 1991; Craig et al. 1993; Geiger et al. 1995; Tsuzuki et al. 2001; Sans et al. 2003). Thus, it seems that the preferred subunit combination in pyramidal cells is GluA1/A2 with additional GluA2/A3 (Geiger et al. 1995; Wenthold et al. 1996; Tsuzuki et al. 2001; Sans et al. 2003; Lu et al. 2009). In contrast, GluA2-lacking Ca^{2+}-permeable AMPARs are expressed preferentially in GABAergic interneurons and play crucial roles in synaptic plasticity and neuronal development (McBain and Dingledine 1993; Geiger et al. 1995; Koh et al. 1995b). Thus, synaptic AMPAR subunits show distinct, yet often overlapping, expression patterns that allow for subunit-specific function and regulation.

Consistent with previous studies (Keinanen et al. 1990; Pellegrini-Giampietro et al. 1991; Lambolez et al. 1992; Petralia et al. 1997), our FISH analyses have shown that cerebellar Purkinje cells (PC) express high levels of GluA2 and GluA3 mRNAs, with low levels of GluA1 mRNA (Fig. 1e–g), whereas molecular layer interneurons (MLIs; i.e., basket and stellate cells) express GluA2–4 mRNAs (Fig. 1f–h). These distinct combinations are also observed in quantitative immunogold EM analyses using subunit-specific antibodies for GluA1–4 (Fig. 2c–f). Considering that AMPAR-mediated EPSCs in PCs show little rectification and low Ca^{2+} permeability (Tempia et al. 1996; Momiyama et al. 2003), the majority of AMPARs there should contain GluA2. Therefore, it seems that the major AMPAR configuration in PCs is GluA2/A3 channels with additional GluA1/A2 channels. By contrast, synapses on MLIs exhibit inwardly rectifying EPSCs under resting conditions, indicating a predominance of GluA2-lacking Ca^{2+}-permeable AMPARs (Liu and Cull-Candy 2000). These AMPARs consist predominantly of GluA3 homomeric channels (Keinanen et al. 1990; Sato et al. 1993) with the additional participation of GluA4 subunits (Gardner et al. 2005). However, high frequency activity at these "Ca^{2+}-permeable synapses" produces a rapid switching from largely GluA2-lacking to GluA2-containing AMPARs (Liu and Cull-Candy 2000; Kelly et al. 2009). Thus, each cell type expresses distinct sets of GluA subunits with differential relative abundance, presumably reflecting cell type-dependent differences in the preferred subunit composition of AMPA receptors.

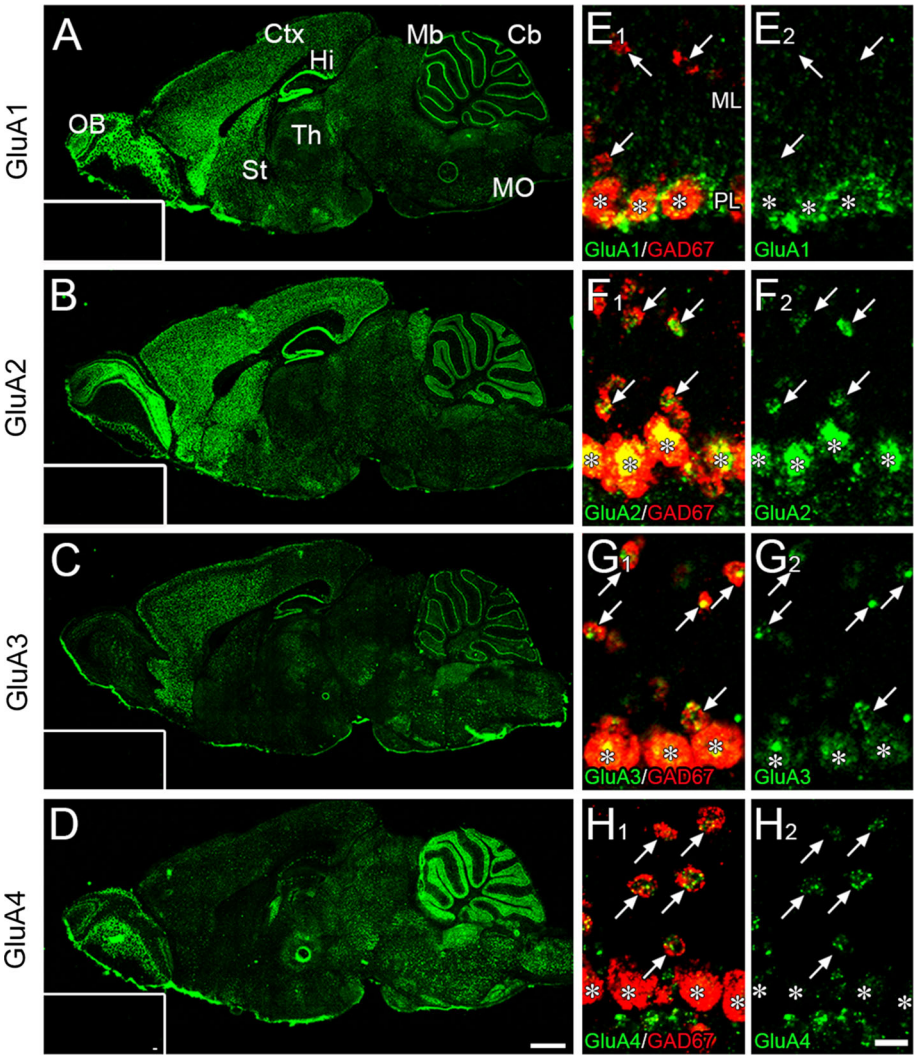

Fig. 1a–h Fluorescent in situ hybridization (FISH) showing distinct patterns of GluA mRNA expression in cerebellar Purkinje cells (PC) and molecular layer interneurons (MLI). **a–d** Single FISH for GluA1–4 in the adult mouse brain. Hybridization with sense probes gives no significant signals (*insets*). **e–h** Double FISH for GluA1–4 (*green*) and GAD67 (*red*) mRNAs in the cerebellar molecular layer. GluA1 mRNA is weak in GAD67 mRNA-positive large cells in the PC layer (*PL*; *asterisks*), and almost absent in GAD67-positive small cells in the molecular layer (*ML*; *arrows*) (**e**). GluA2 mRNA is expressed at consistently high levels in PCs, whereas it is expressed at variable levels in MLIs (**f**). GluA3 mRNA is expressed in PCs and MLIs (**g**). GluA4 mRNA is expressed moderately in MLIs (**h**). Small cells expressing high levels of GluA1 and GluA4 mRNAs are identified as Bergmann glia cells, because these hybridizing signals overlap with those for the glutamate transporter GLAST, which are enriched in these glia (data not shown). *OB* Olfactory bulb, *Ctx* cerebral cortex, *St* striatum, *Hi* hippocampus, *Th* thalamus, *Mb* midbrain, *Cb* cerebellum, *MO* medulla oblongata, *ML* molecular layer, *PL* Purkinje cell layer. *Bars*: (in **d**) **a–d** 1 mm; (in $\mathbf{h}_2$) **e–h** 10 μm. Reproduced with permission from Yamasaki et al. (2011)

Considering that individual neurons in the brain typically receive synaptic inputs from multiple sources, the question arises whether different GluA subunits can be associated selectively with functionally distinct inputs. For example, in hippocampal CA3 interneurons, GluA2-lacking and GluA2-containing AMPARs are segregated to synapses from mossy fibers and CA3 recurrent collaterals, respectively (Toth and McBain 1998). Differential allocation of GluA subunits is also observed in fusiform cells of the dorsal cochlear nucleus: GluA2 is expressed at both parallel and auditory fiber synapses on apical dendrites, whereas GluA4 is limited to auditory fiber synapses on basal dendrites (Rubio and Wenthold 1997). However, this is not the case for cerebellar PC synapses. PCs receive two distinct excitatory afferents: numerous parallel fibers (PFs) and a single climbing fiber (CF) (Palay and Chan-Palay 1974). To distinguish these inputs, we employed double immunogold labeling for GluA subunits and terminal markers (Fig. 2a, b): VGluT1 for PF terminals and VGluT2 for CF terminals (Miyazaki et al. 2003). Quantitative immunogold EM analysis revealed that, in each of GluA1–3, the ratio of the labeling density between CF

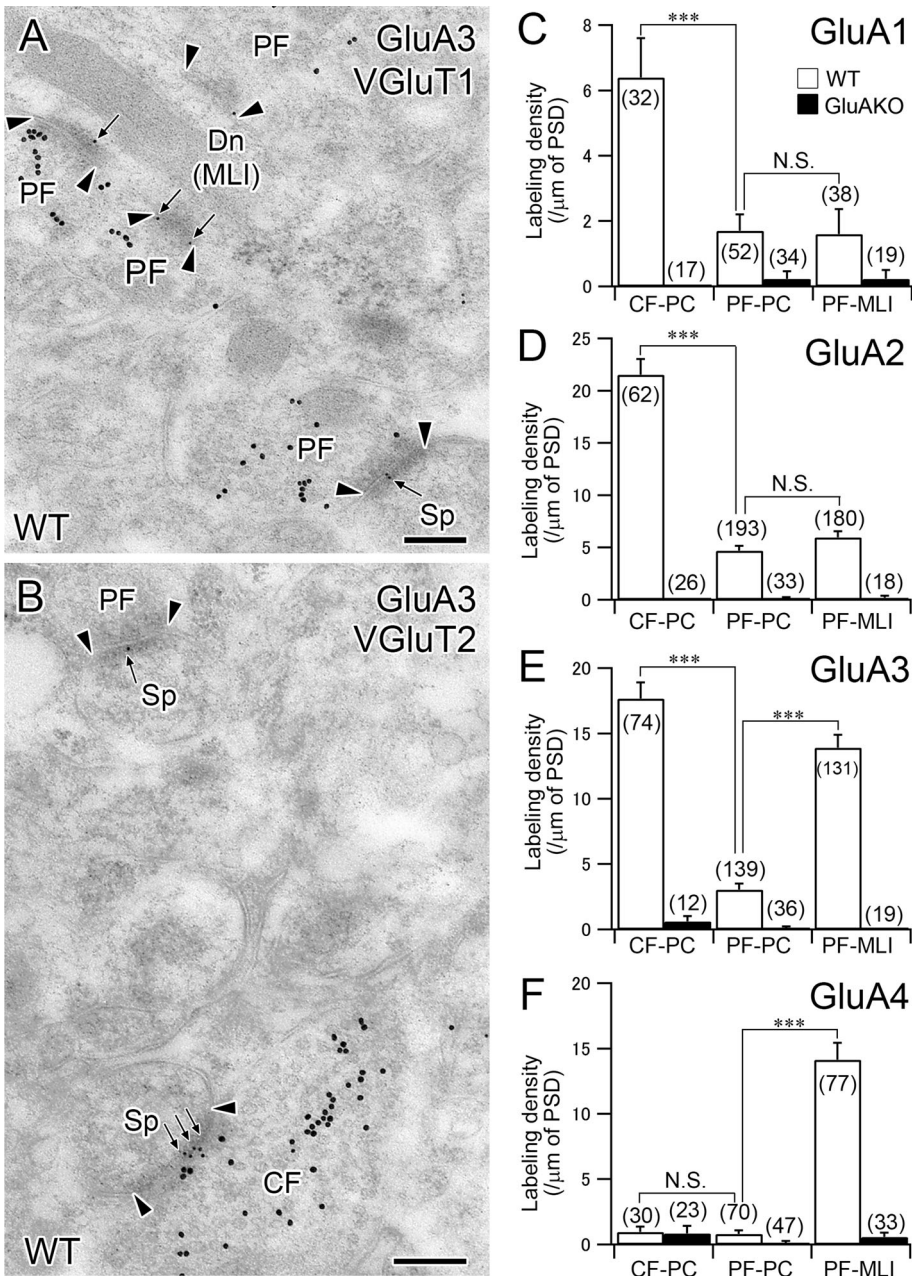

Fig. 2a–f Postsynaptic labeling for GluA1–4 at three types of cerebellar synapses in wild-type mice. Quantitative immunogold EM analyses on the labeling density of GluA1–4 at three types of excitatory synapses in the cerebellar molecular layer. **a** Double-labeling postembedding immunogold EM for GluA3 ($\phi = 10$ nm) and VGluT1 ($\phi = 15$ nm). Asymmetrical synapses between VGluT1-labeled PF terminal (*PF*) and PC spine (*Sp*), and those between PF terminal and dendritic shaft of MLIs [Dn (MLI)] are labelled only occasionally for GluA3 (*arrows*). **b** Double-labeling postembedding immunogold EM for GluA3 ($\phi = 10$ nm) and VGluT2 ($\phi = 15$ nm). GluA3 labeling at synapses between the VGluT2-labeled CF terminal (*CF*) and PC spine (*Sp*) is clearly higher than that in VGluT2-unlabeled PF-PC synapses. **c–f** Quantitative immunogold EM analyses on the labeling density of GluA1–4 at three types of excitatory synapses in the cerebellar molecular layer. Note that the preferred GluA subunit combination is GluA1–3 and GluA2–4 at PF-PC and CF-PC synapses, and PF-MLI synapses, respectively. The specificity of postsynaptic labeling for each GluA subunit is confirmed by the almost blank labeling in control GluA-KO mice (*black bars*). *Error bars* represent SEM. *Numbers* of analyzed synapses are indicated in *parentheses*. Mann–Whitney *U* test; $***P < 0.001$; *NS* not significant ($P > 0.05$). *Bars* 200 nm. Edges of postsynaptic density (PSD) are indicated by *arrowheads*. Reproduced with permission from Yamasaki et al. (2011)

synapses and PF synapses is similar (Fig. 2c–e, white bars; Table 1). Thus, there would be no obvious difference in the relative abundance of the four GluA subunits, indicating that subunit combinations at PC synapse is determined primarily in a cell type-dependent manner with little input-dependent difference.

Table 1 Densities of immunogold particles for GluA1–4 [particles/1 μm of postsynaptic density (PSD)] in control and GluD2-KO mice. Statistical significance between the wild-type control and GluD2-KO mice was assessed by Mann–Whitney *U*-test. *SD* Standard deviation, *N* number synapses examined

Control			GluD2-KO			
GluA1	Mean ± SD	*N*	GluA1	Mean ± SD	*N*	*P*
CF-PC	6.3 ± 6.9	32	CF-PC	5.0 ± 6.5	54	0.38
PF-PC	1.7 ± 3.7	52	PF-PC	5.0 ± 6.3	47	2.01×10^{-3}**
PF-Int	1.6 ± 4.7	38	PF-Int	1.0 ± 2.9	56	0.53
GluA2	Mean ± SD	*N*	GluA2	Mean ± SD	*N*	*P*
CF-PC	21.5 ± 11.5	62	CF-PC	19.9 ± 12.4	96	0.38
PF-PC	4.7 ± 6.5	193	PF-PC	14.1 ± 9.2	133	7.58×10^{-20}***
PF-Int	6.0 ± 7.7	180	PF-Int	12.2 ± 11.1	204	2.89×10^{-10}***
GluA3	Mean ± SD	*N*	GluA3	Mean ± SD	*N*	*P*
CF-PC	17.7 ± 10.6	74	CF-PC	15.9 ± 11.7	77	0.32
PF-PC	3.0 ± 5.5	139	PF-PC	17.0 ± 11.4	91	6.54×10^{-9}***
PF-Int	14.0 ± 11.2	131	PF-Int	23.5 ± 16.6	133	9.26×10^{-8}***
GluA4	Mean ± SD	*N*	GluA4	Mean ± SD	*N*	*P*
CF-PC	1.0 ± 2.3	30	CF-PC	0.5 ± 2.0	31	0.39
PF-PC	0.8 ± 2.3	70	PF-PC	0.2 ± 0.8	33	0.07
PF-Int	14.2 ± 11.3	77	PF-Int	14.8 ± 9.9	55	0.73

** $P < 0.01$; *** $P < 0.001$

Quantitative difference in AMPAR expression

Another fundamental issue regarding the distribution of synaptic glutamate receptors is whether every synapse contains the same number or density of receptors. In contrast to the density of $GABA_A$ receptors, which has been shown to be uniform among cerebellar PCs, stellate cells, and dentate granule cells (Nusser et al. 1997), that of AMPARs is highly variable among different types of synapses (Nusser et al. 1998; Fukazawa and Shigemoto 2012). For example, in hippocampal CA3 pyramidal cells, mossy fiber synapses have approximately four times more AMPARs than associational/commissural fiber (A/C) synapses, suggesting input pathway-dependent regulation (Nusser et al. 1998). However, A/C synapses on interneurons have four times more AMPARs than those on pyramidal cells in the hippocampal CA3 area, suggesting target cell type-dependent regulation (Nusser et al. 1998). Likewise, individual AMPAR subunits in cerebellar molecular layer synapses are also regulated in an input pathway- and target cell type-dependent manner. In PCs, synapses from PFs have four times more AMPARs than those from CFs (Masugi-Tokita et al. 2007; Yamasaki et al. 2011). Furthermore, PF synapses on MLIs have four times more AMPARs than those on PCs (Masugi-Tokita et al. 2007). In PCs, the density of postsynaptic labeling for GluA1–3 at PF synapses is four to six times lower than that at CF synapses (Fig. 2c–e, white bars; Table 1). This trend is also observed between PF synapses on PCs and MLIs, where the labeling density for GluA3 is four times higher at PF-MLI synapses than at PF-PC synapses (Fig. 2e, white bars; Table 1).

Input pathway-dependent regulation of synaptic AMPAR in cerebellar PCs requires GluD2

What then are the molecular mechanisms underlying this skewed distribution of synaptic AMPARs? From multiple lines of evidence, we hypothesized that GluD2 (GluRδ2) could be involved in the input pathway-dependent selective abundance of AMPARs at PF-PC synapses. In cerebellar PCs, the glutamate receptor GluD2 is expressed selectively at PF synapses but not at CF synapses (Takayama et al. 1996; Landsend et al. 1997) (Fig. 3). GluD2 plays an essential role in the formation and maintenance of PF-PC synapses (Kashiwabuchi et al. 1995; Kurihara et al. 1997; Lalouette et al. 2001; Takeuchi et al. 2005; Uemura et al. 2007; Matsuda et al. 2010). Furthermore, GluD2 regulates endocytosis of AMPARs (Hirai et al. 2003) and mediates LTD at PF-PC synapses (Kashiwabuchi et al. 1995). To explore this possibility, we applied postembedding immunogold EM to GluD2-knock out (KO) and control mice, and measured the labeling density for GluA1–4 (Fig. 4; Table 1). In GluD2-KO mice, GluA1–3 shows a marked (three- to four-fold) increase at PF-PC, but not CF-PC, synapses (Fig. 4c–e, left and middle). Consequently,

input pathway-dependent distribution of synaptic AMPARs in control PCs is almost eliminated in GluD2-KO PCs (Fig. 4c–e, gray bars). Unexpectedly, a modest (two-fold) increase of GluA2 and GluA3, but not GluA4, is also found at PF synapses in MLIs (Fig. 4d–f, right), where we identified a low but significant expression of GluD2 (Fig. 3e, right). These results indicate that GluD2 is involved in a common mechanism that suppresses the synaptic expression of particular GluA subunits at PF synapses in PCs and MLIs.

During long-term depression (LTD) at PF-PC synapses, the number of postsynaptic AMPARs is reduced by endocytosis (Matsuda et al. 2000; Wang and Linden 2000). Interestingly, application of an antibody against the putative ligand-binding domain of GluD2 induces AMPAR endocytosis, attenuates synaptic transmission, and impairs PF-LTD in cultured PCs (Hirai et al. 2003). From this evidence, it is possible to speculate that increased AMPAR expression could result from impaired PF-LTD in GluD2-KO mice (Kashiwabuchi et al. 1995). However, there is no significant increase in the density of GluA2 labeling in two major PF-LTD-deficient models: mGluR1-KO mice (Aiba et al. 1994) and GluD2ΔT mice, which lack the membrane-proximal domain of the C-terminal region of GluD2 (Uemura et al. 2007). Thus, the increase in synaptic AMPARs is not common to PF-LTD-deficient mutants, but specific to GluD2-KO mice. The other possibility is that GluD2 at PF synapses delimits the number of synaptic slots available for AMPARs. In the hippocampus, the specific interaction between PSD-95 and transmembrane AMPAR regulatory proteins (TARPs) has been shown to determine the number of synaptic AMPARs (Schnell et al. 2002; Stein et al. 2003; Ehrlich and Malinow 2004). In GluD2-KO mice, PSD-93 and PSD-95 at PF-PC synapses display concomitant increases, suggesting an increased capacity for AMPAR-TARP complexes. Compared with AMPARs, GluD2 is transported to the cell surface much more efficiently, in part, due to a strong endoplasmic reticulum exit signal in the C-terminal domain (Matsuda and Mishina 2000; Yuzaki 2009; Matsuda et al. 2010). Therefore, GluD2 appears to play a key role in the regulation of postsynaptic molecular organization and may delimit the number of slots available for AMPARs at PF synapses.

Although our data indicate that GluD2 plays an essential role in regulating the number of synaptic AMPARs at PF synapses, other mechanisms have been proposed to influence the membrane trafficking and synaptic targeting of AMPARs, including their C-terminal tail interactions with various synaptic molecules (Ziff 2007; Jackson and Nicoll 2011). These alternative processes may have distinct or synergistic functions in the regulation of synaptic AMPARs at cerebellar synapses. Thus, the amount and density, as well as subunit composition, of AMPA receptors at a given glutamatergic synapse is governed by both pre- and postsynaptic factors, resulting in functionally distinct connections.

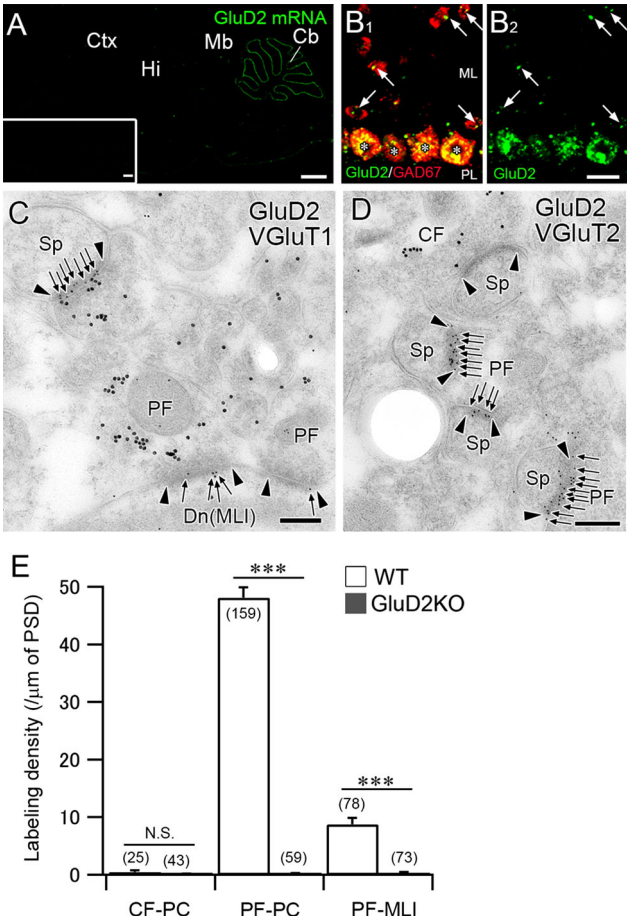

Fig. 3a–e GluD2 mRNA and protein is expressed predominantly in PCs and additionally in MLIs. **a** FISH showing exclusive expression of GluD2 mRNA (*green*) in the cerebellum in the adult mouse brain. Note that the sense probe yields no specific labeling (*inset*). **b** Double-labeling FISH for GluD2 (*green*) and GAD67 (*red*) mRNAs. In addition to strong labeling in PCs (*asterisks*), GAD67 mRNA-positive *MLIs* in the molecular layer (*arrows*) are labeled consistently for one of two tiny punctate signals for *GluD2* mRNA. **c**, **d** Double labeling postembedding immunogold EM for *GluD2* ($\phi = 10$ nm) and terminal markers ($\phi = 15$ nm: *VGluT1* in **c**, *VGluT2* in **d**). *GluD2* is localized exclusively at *VGluT1*-positive *PF-PC* synapses (**c**), but not in *VGluT2*-positive *CF-PC* synapses (**d**). *PF-MLI* synapses are moderately labeled for *GluD2* (**c**). **e** *Histograms* showing labeling density for *GluD2* at three excitatory synapses in control (*white bars*) and GluD2-KO (*black bars*) mice. On average, the density of immunogold labeling at *PF-MLI* synapses amounts to 20 % of that at *PF-PC* synapses. *Error bars* Standard error of the mean (SEM). Numbers of synapses examined are indicated in *parentheses*. $***P < 0.0001$, Mann–Whitney *U* test. *NS* Not significant. *Bars* **a** 1 mm; **b** 10 μm; **c**, **d** 200 nm. Reproduced with permission from Yamasaki et al. (2011)

Target cell type- and pathway-dependent regulation of NMDAR expression

Qualitative differences in NMDAR expression

NMDARs are the most important trigger for the activity-dependent long-term modification of synaptic strength (Lisman 1989; Bliss and Collingridge 1993; Cull-Candy et al. 2001), and their distribution also seems to be regulated by pre- and post-synaptic factors. Classical NMDARs consist of the obligatory subunit GluN1 (GluRζ1 or NR1) and any of the four regulatory GluN2 subunits (GluRε or NR2) (Seeburg 1993; Nakanishi and Masu 1994; Mori and Mishina 1995). Most of the diversity in the biophysical properties of NMDARs arises from the GluN2 subunit composition (Cull-Candy et al. 2001). GluN2 subunit expression displays a unique spatiotemporal profile (Lambolez et al. 1992; Watanabe et al. 1992; Monyer et al. 1994; Cull-Candy et al. 2001). For example, GluN2B (GluRε2 or NR2B) is expressed widely during prenatal development, whereas it is restricted to the forebrain in the adult brain. In sharp contrast, GluN2A (GluRε1 or NR2A) expression is ubiquitous in the CNS, starting at very low levels around the time of birth, and increasing dramatically during the second postnatal week. GluN2C (GluRε3 or NR2C) expression is first detected during the second

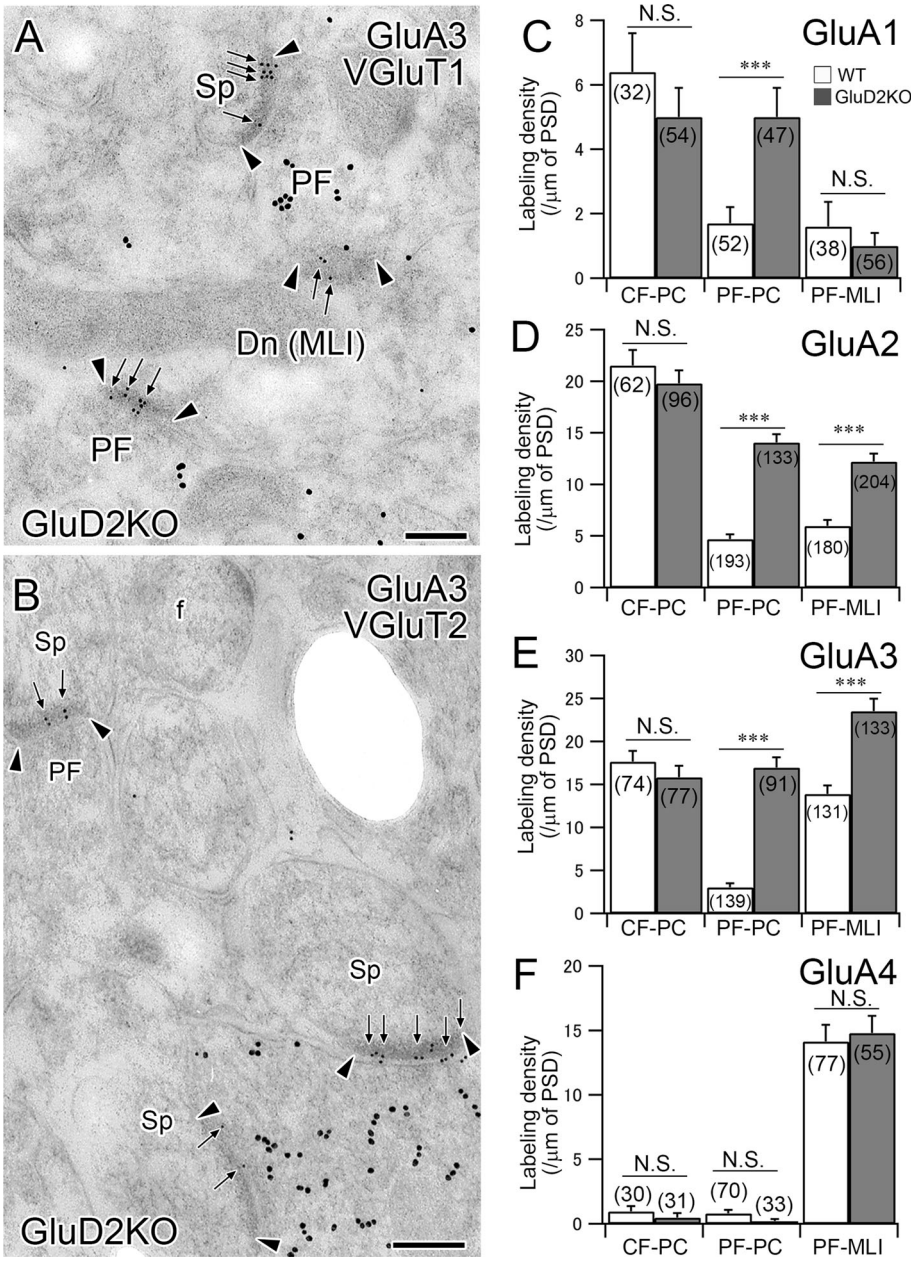

Fig. 4a–f Comparing the labeling density of GluA1–4 at three types of cerebellar synapses in the wild-type and *GluD2-KO* mice. **a**, **b** Double-labeling postembedding immunogold for *GluA3* (ϕ = 10 nm) and *VGluT1* (ϕ = 15 nm) or *VGluT2* (ϕ = 15 nm). In GluD2-KO mice, while *GluA3* labeling at *PF-PC* synapses is increased robustly (**a**, **b**), that at *CF-PC* synapses remains unaffected (**b**). **c**–**f** Quantitative immunogold EM analyses. Note that in GluD2-KO mice, the labeling density of GluA1–3 shows a three- to four-fold increase at PF-PC synapses, but not at *CF-PC* synapses. In addition, the labeling density of GluA2 and GluA3, but not GluA4, at PF-MLI synapses shows a two-fold increase. *Error bars* represent SEM. Numbers of synapses examined are indicated in *parentheses*. ***$P < 0.0001$, Mann–Whitney *U* test. *NS* not significant. *Scale bars* 200 nm. Edges of PSD are indicated by *arrowheads*. Reproduced with permission from Yamasaki et al. (2011)

postnatal week, and is highly enriched in the adult cerebellum. GluN2D (GluRε4 or NR2D) is expressed widely in early development, but is restricted to the brainstem and spinal cord in adulthood (Watanabe et al. 1992; Monyer et al. 1994).

GluN2A and GluN2B have received considerable attention over the past few decades, because these subunits are expressed highly in the cortex and hippocampus, and play a central role in synaptic plasticity and metaplasticity. For example, GluN2A replaces GluN2B in an activity-dependent manner (Barria and Malinow 2002), and the ratio of GluN2A to GluN2B is considered one of the crucial factors dictating the polarity of synaptic plasticity (Collingridge et al. 2004). In hippocampal CA3 pyramidal neurons in adulthood, these subunits are segregated to distinct synapses; CA3 pyramidal cell synapses from A/C input contain GluN1 and GluN2A and GluN2B, whereas synapses from mossy fibers contain only GluN1 and GluN2A (Fritschy et al. 1998; Watanabe et al. 1998). Similarly, GluN2B subunit influence at CA1 pyramidal cell synapses has been shown to differ depending on the laterality of origin of input (ipsilateral or contralateral CA3 pyramidal cells) (Kawakami et al. 2003). Therefore, differential allocation of GluN2A- and GluN2B-containing NMDARs is likely to be regulated by several mechanisms depending on the input pathway and neuronal activity.

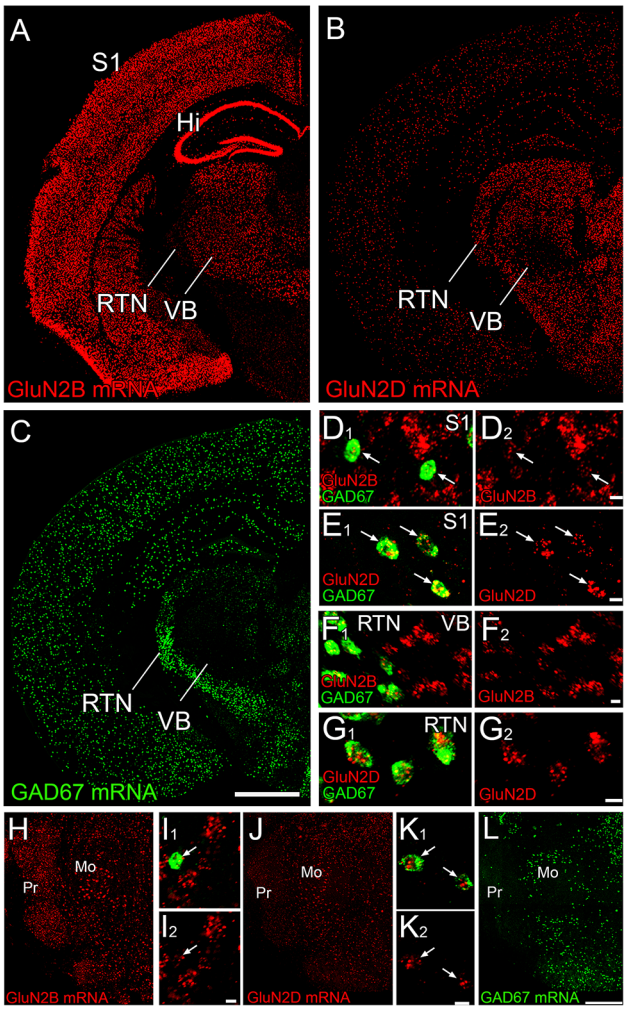

Fig. 5a–l FISH showing distinct neuronal expression of GluN2B and GluN2D mRNAs at trigeminal relay stations in adult mice. **a–c** Overall labeling patterns for mRNAs of GluN2B (**a**), GluN2D (**b**), and GAD67 (**c**) in a coronal forebrain section through the primary somatosensory cortex (*S1*), the ventrobasal thalamic nucleus (*VB*), and reticular thalamic nucleus (*RTN*). **d–g** Double-labeling FISH for GAD67 (*green*; **d–g**) and GluN2B (*red*; **d**, **g**) or GluN2D (*red*; **e**, **g**) mRNAs in the S1 (**d**, **e**), VB and RTN (**f**, **g**). **h–l** Overall labeling patterns for mRNAs of GluN2B (**h**), GluN2D (**j**), and GAD67 (**l**) in a coronal brainstem section through the trigeminal principal sensory nucleus (*Pr*). **I**, **k** Double-labeling FISH for GAD67 (*green*; **I**, **k**) and GluN2B (*red*; **I**) or GluN2D (*red*; **k**) mRNAs in the Pr. Note preferential labeling for GluN2B mRNA in GAD67 mRNA(−) neurons and for GluN2D mRNA in GAD67 mRNA(+) neurons (*arrows*) in both forebrain and brainstem sections. *Hi* Hippocampus, *Mo* trigeminal motor nucleus. *Bars*: **a–c** (in **c**), **h**, **j**, **l** (in **l**) 1 mm; **d–g**, **I**, **k** 10 μm. Reproduced with permission from Yamasaki et al. (2014)

Segregated GluN2B and GluN2D expression in trigeminal relay stations

In fetal and neonatal brains, GluN2B and GluN2D are the major regulatory subunits (Watanabe et al. 1992; Monyer et al. 1994). There are a number of contrasting physiological properties between these subunits, including channel conductance and the duration of channel opening, that might contribute to differential postsynaptic Ca^{2+} influx (Monyer et al. 1994; Misra et al. 2000a, b; Momiyama et al. 2003). Furthermore, GluN2B and GluN2D are organized in a pathway-dependent manner along the trigeminal pathway in both neonatal and adult mice (Yamasaki et al. 2014).

Consistent with previous studies using isotopic ISH (Watanabe et al. 1992; Monyer et al. 1994), FISH analyses have shown that GluN2B mRNA is highly expressed throughout the cortex and thalamus (Fig. 5a), whereas GluN2D mRNA is expressed only sparsely in these regions (Fig. 5b). In the primary somatosensory cortex (S1), GluN2B mRNA is expressed intensely in GAD67 mRNA(−) neurons and weakly in GAD67 mRNA(+) neurons (Fig. 5d), whereas GluN2D mRNA expression is restricted to GAD67 mRNA(+) neurons (Fig. 5e). In the thalamic ventrobasal (VB) complex, GluN2B mRNA expression is high in neurons lacking GAD67 mRNA, whereas it is low in reticular thalamic nucleus (RTN) neurons expressing GAD67 mRNA (Fig. 5f). In contrast, GluN2D mRNA expression is selective to RTN neurons expressing GAD67 mRNA (Fig. 5g). This pattern of neuronal expression is also found in the principal sensory nucleus of the trigeminal nucleus (Pr; Fig. 5h–l). Thus, it is common to each somatosensory station that non-

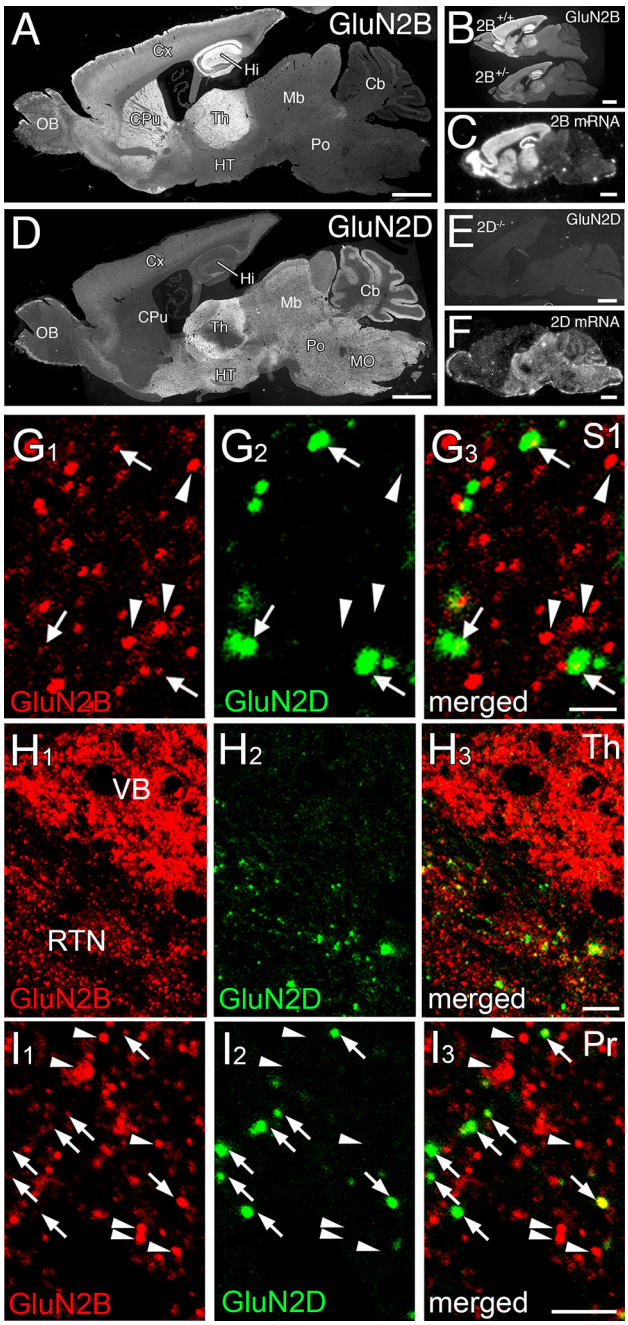

◀**Fig. 6a–I** Immunofluorescence showing the distinct distribution patterns of GluN2B and GluN2D immunoreactivities at trigeminal relay stations in adult mice. **a**, **d** Overall staining patterns in wild-type mouse brains for GluN2B (**a**) and GluN2D (*D*). **b**, **e** The specificity is indicated by substantial reduction of GluN2B immunolabeling in the GluN2B$^{+/-}$ brain compared with the GluN2B$^{+/+}$ brain (**b**), and by the lack of GluN2D immunolabeling in the GluN2D$^{-/-}$ brain (**e**). **c, f** Isotopic in situ hybridization for GluN2B (**c**) and GluN2D (**f**) mRNAs in adult mouse brains. **g–I** High-power views of double immunofluorescence for GluN2B (*red*) and GluN2D (*green*) in the S1 (**g**), VB and RTN (**h**), and Pr(**I**). Intense GluN2B-positive puncta virtually lack GluN2D signals (*arrowheads*), and GluN2D puncta often possess weak GluN2B signals (*arrows*). *Cb* Cerebellum, *CPu* caudate-putamen, *Cx* cortex, *Hi* hippocampus, *HT* hypothalamus, *Mb* midbrain, *MO* medulla oblongata, *OB* olfactory bulb, *Po* pons, *Th* thalamus. *Bars*: **a–f** 1 mm; **g** 2 μm; **h** 10 μm; **I** 5 μm. Reproduced with permission from Yamasaki et al. (2014)

GABAergic, most likely glutamatergic, neurons express GluN2B mRNA exclusively, whereas GABAergic neurons express GluN2D mRNA at high levels and GluN2B mRNA at low levels.

GluN2B and GluN2D protein localization is almost segregated along the trigeminal pathway. Immunofluorescence using parasagittal sections has revealed predominant immunolabeling of GluN2B and GluN2D proteins in the forebrain or brainstem, respectively (Fig. 6a, d), which is consistent with their distinct mRNA expressions (Fig. 6c, f). Double immunofluorescence shows that bright GluN2B(+) puncta lack detectable signals for GluN2D, whereas bright GluN2D(+) puncta show weak signals for GluN2B (Fig. 6g). The VB is crowded with bright GluN2B(+) puncta lacking GluN2D(+) immunoreactivity, whereas bright GluN2D(+) puncta in the RTN have weak immunoreactivity for GluN2B (Fig. 6h). A similar trend is also observed in the Pr (Fig. 6i). Further postembedding immunogold EM analyses revealed that GluN2B and GluN2D are specifically localized to asymmetrical synapses in each adult trigeminal relay station (S1, Fig. 7; PrV, VB, data not shown). Because GABA is contained in dendrites as well as the axon terminals of GABAergic neurons (Bolam et al. 1983), GABA can be used as a GABAergic dendritic marker (Fig. 7). Both subunits are detected preferentially on the postsynaptic membrane of asymmetrical synapses in the S1 (Fig. 7a, b). The density of GluN2B labeling per 1 μm of the postsynaptic density is three times higher at synapses on GABA(−) dendrites (mostly on dendritic spines) than synapses on GABA(+) dendrites (mostly on dendritic shafts) (Fig. 7c, left; $P < 0.001$, *U* test). By contrast, the density of GluN2D labeling is five times higher at synapses on GABA(+) dendrites than synapses on GABA(−) dendrites, and the density of the latter is almost comparable to the background labeling as determined from the corresponding synapses in GluN2D$^{-/-}$ mice (Fig. 7d, left; $P < 0.001$, *U* test). Similar segregated synaptic distribution is also observed in the Pr and spinal trigeminal subnucleus interpolaris (SpVi) (Fig. 7c, d, middle and right). Therefore, GluN2B is predominantly expressed at asymmetrical synapses on glutamatergic neurons, whereas GluN2D is selective to asymmetrical synapses on GABAergic neurons at each trigeminal station.

To investigate the functional significance of segregated GluN2B and GluN2D expression in the trigeminal somatosensory pathway, we examined the formation and maturation of whisker-related patterning in GluN2B$^{+/-}$

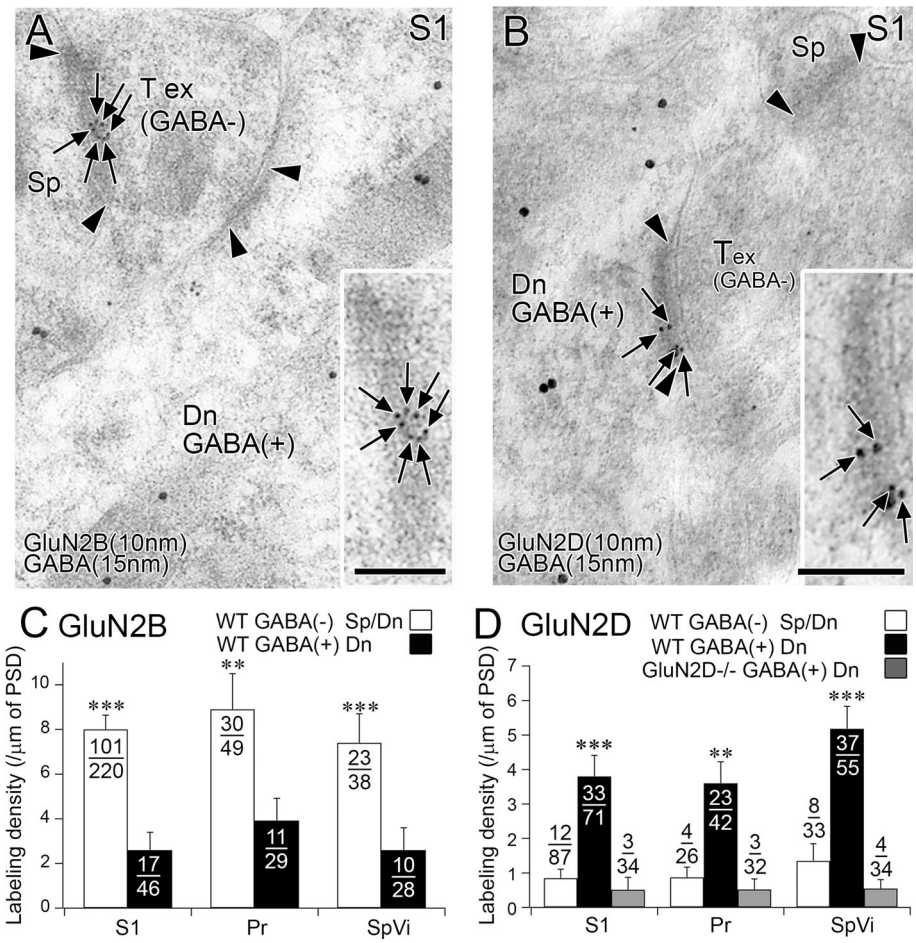

Fig. 7a–d Postembedding immunogold EM showing distinct postsynaptic expression of GluN2B and GluN2D at relay stations of the adult trigeminal pathway. **a**, **b** Double-labeling postembedding immunogold EM for GABA ($\phi = 15$ nm) and GluN2B ($\phi = 10$ nm; **a**) or GluN2D ($\phi = 10$ nm; **b**) in the S1. GluN2B is preferentially expressed at asymmetrical synapses on GABA(−) dendritic shaft and spines, and GluN2D is at GABA(+) dendrites. **c, d** Summary bar graphs representing preferential expression of GluN2B (**c**) and GluN2D (**d**) at synapses on GABA(−) and GABA(+) postsynaptic compartments in the S1, Pr, and SpVi. The background level of GluN2D labeling was measured at synapses on GABA-positive dendrites in GluN2D$^{-/-}$ mice. *Arrowhead* indicates the edge of the postsynaptic density. *Error bars* SEM. The ratio of labeled synapses to the total number of synapses examined is indicated as a fraction in each column. $^{**}P < 0.01$ (*U* test). $^{***}P < 0.001$ (*U* test). *Dn* Dendrite; *Sp* spine; *T ex* GABA-negative (excitatory) terminal, *T in* GABA-positive (inhibitory) terminal. *Bars* 200 nm. Reproduced with permission from Yamasaki et al. (2014)

and GluN2D$^{-/-}$ mice. Because GluN2B$^{-/-}$ mice display neonatal lethality (Kutsuwada et al. 1996), we instead analyzed GluN2B$^{+/-}$ mice, which have half the amount of GluN2B protein compared with control mice. To visualize whisker-related patterning, cytochrome oxidase (CO) histochemistry was applied to brain samples from GluN2B$^{+/-}$, GluN2D$^{-/-}$, and control littermates. In control mice, barrels in the S1 are obscure in all pups at P3, with segregated barrels appearing after P4 (Fig. 8a, e for GluN2B$^{+/+}$ mice; Fig. 8c, g for GluN2D$^{+/+}$ mice). In comparison, the appearance of barrels was delayed in GluN2B$^{+/-}$ mice (Fig. 8b, f, I) and advanced in GluN2D$^{-/-}$ mice (Fig. 8d, h, j). The termination stage of critical period plasticity, as assessed by CO histochemistry 8 days (S1) after transection of the right ION, displays similar temporal shifts. In control mice, ION transection at P3 substantially lowers overall CO intensity and blurs patterning in the contralateral hemisphere (Fig. 8k, m). By contrast, critical period plasticity termination is delayed in GluN2B$^{+/-}$ mice (Fig. 8p, s) and advances in GluN2D$^{-/-}$ mice (Fig. 8n, t). Thus, the refinement of whisker-related maps, assessed by the appearance of cortical barrels and termination of lesion-induced critical period plasticity, is delayed by nearly a day in the somatosensory cortex of GluN2B$^{+/-}$ mice but advanced by nearly a day in GluN2D$^{-/-}$ mice. These findings indicate the possibility that pathway-dependent organization of GluN2B and GluN2D-containing NMDARs is required for positive and negative modulation of somatosensory development and maturation, respectively.

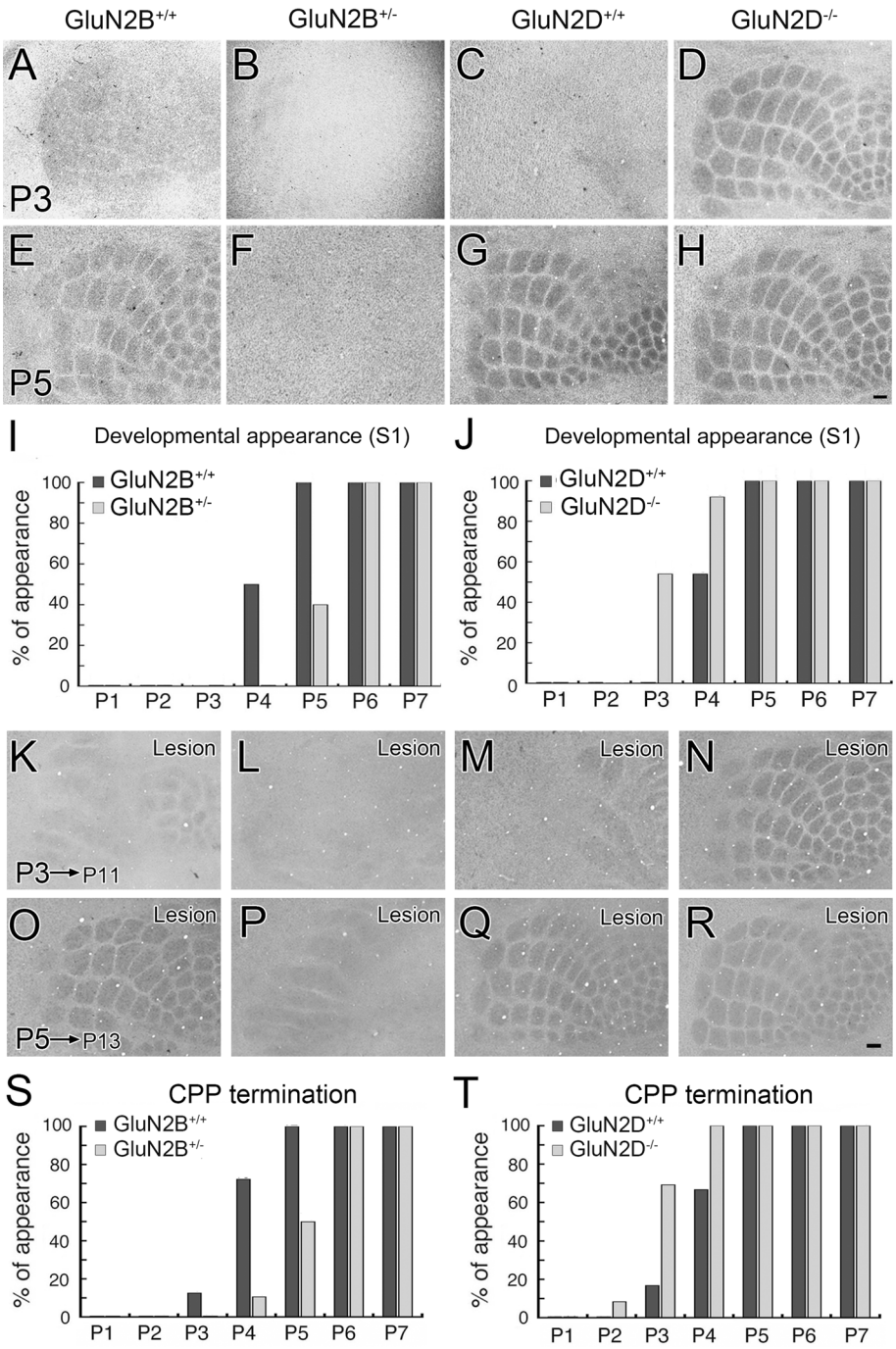

Fig. 8 Developmental appearance and termination of lesion-induced critical period plasticity in cortical barrels is delayed in GluN2B$^{+/-}$ mice and advanced in Glu2D$^{-/-}$ mice. **a**–**h**, Cytochrome oxidase (CO) histochemistry on flattened cortical sections at P3 (**a**–**d**), and P5 (**e**–**h**). **I**, **j** *Bar graphs* showing the 1 day delay of barrel appearance in GluN2B$^{+/-}$ mice (**I**) and 1 day advance in GluN2D$^{-/-}$ mice (**j**). **k**–**t** The right infraorbital nerve was transected at P3 (**k**–**n**), and P5 (**o**–**r**), and CO histochemistry was applied 8 days later. **s**, **t** *Bar graphs* representing the 1 day delay of critical period plasticity (CPP) termination in GluN2B$^{+/-}$ mice (**s**) and 1 day advance in GluN2D$^{-/-}$ mice (**t**). *Bars* 100 μm. Reproduced with permission from Yamasaki et al. (2014)

Quantitative differences in NMDAR expression

Compared with AMPARs, the synaptic content of NMDARs is much less variable between individual synapses (Racca et al. 2000; Nimchinsky et al. 2004; Noguchi et al. 2005; Sobczyk et al. 2005). For example, only ~80 % of Schaffer collateral synapses onto CA1 pyramidal cell spines have a detectable number of AMPARs (Nusser et al. 1998; Takumi et al. 1999; Racca et al. 2000) and display a highly skewed distribution. By contrast, virtually all of these synapses contain immunoreactive NMDARs with small variability (Takumi et al. 1999; Racca et al. 2000). Specifically, Racca et al. (2000) showed that in CA1 pyramidal cell A/C synapses, the variability in synaptic NMDAR content [coefficient of variation (CV), 0.64–0.70] is much lower than that of the AMPAR content (CV 1.17–1.45). Furthermore, as there is no significant difference in the labeling of the obligatory NR1 subunit among synapses receiving different input sources, the net expression level of NMDAR is less likely to undergo input-specific regulation (Nyiri et al.

2003). Instead, CA1 parvalbumin (PV)-positive interneuron synapses display much lower labeling density of NR1 subunits than pyramidal cell synapses, showing a cell-type specific difference (Nyiri et al. 2003). Thus, it seems that postsynaptic cell types affect the synaptic NMDAR content, whereas presynaptic inputs are related to the distinct composition of NMDARs.

Conclusions

In summary, the above molecular-anatomical evidence has established that the synaptic allocation of AMPARs and NMDARs is regulated in an input pathway- and target cell type-dependent manner, and that it is essential for the proper functioning of neural circuits. There are, however, important questions that arise from these findings. How are these distributions regulated by neuronal activity? What are the underlying upstream and downstream molecular mechanisms? Furthermore, compared with the density or number of synaptic glutamate receptors, much less is known about subsynaptic distribution on the two-dimensional synaptic face, which also offers a powerful level of regulation over synaptic strength. Thus, it is essential to identify correlations between the functional properties and the molecular characteristics of glutamatergic synaptic connections. Knowledge gained through such studies will greatly facilitate our understanding of how these fine-tuned glutamatergic connections are established.

Acknowledgments I would like to thank Prof. Masahiko Watanabe and my colleagues at the Department of Anatomy, Hokkaido University Graduate School of Medicine for their discussions and collaboration. This work was supported in part by a Grant-in-Aid for Scientific Research (24790187) from the Ministry of Education, Culture, Sports, Science and Technology, and a research grant from the Naito Foundation. The author received the Encouragement Award of the Japanese Association of Anatomists for fiscal year 2014, and gave a presentation of the present review at the 120th Annual Meeting in Kobe, Japan.

Compliance with ethical standards

Conflict of interest The author declares that there are no conflicts of interest.

References

Aiba A, Kano M, Chen C, Stanton ME, Fox GD, Herrup K, Zwingman TA, Tonegawa S (1994) Deficient cerebellar long-term depression and impaired motor learning in mGluR1 mutant mice. Cell 79:377–388

Barria A, Malinow R (2002) Subunit-specific NMDA receptor trafficking to synapses. Neuron 35:345–353

Bliss TV, Collingridge GL (1993) A synaptic model of memory: long-term potentiation in the hippocampus. Nature 361:31–39

Bolam JP, Clarke DJ, Smith AD, Somogyi P (1983) A type of aspiny neuron in the rat neostriatum accumulates [3H] γ-aminobutyric acid: combination of Golgi-staining, autoradiography, and electron microscopy. J Comp Neurol 213:121–134

Borges K, Dingledine R (1998) AMPA receptors: molecular and functional diversity. Prog Brain Res 116:153–170

Bowie D, Mayer ML (1995) Inward rectification of both AMPA and kainate subtype glutamate receptors generated by polyamine-mediated ion channel block. Neuron 15:453–462

Bredt DS, Nicoll RA (2003) AMPA receptor trafficking at excitatory synapses. Neuron 40:361–379

Brunel N, Hakim V, Isope P, Nadal JP, Barbour B (2004) Optimal information storage and the distribution of synaptic weights: perceptron versus Purkinje cell. Neuron 43:745–757

Collingridge GL, Isaac JT, Wang YT (2004) Receptor trafficking and synaptic plasticity. Nat Rev Neurosci 5:952–962

Collingridge GL, Olsen RW, Peters J, Spedding M (2009) A nomenclature for ligand-gated ion channels. Neuropharmacology 56:2–5

Craig AM, Blackstone CD, Huganir RL, Banker G (1993) The distribution of glutamate receptors in cultured rat hippocampal neurons: postsynaptic clustering of AMPA-selective subunits. Neuron 10:1055–1068

Cull-Candy S, Brickley S, Farrant M (2001) NMDA receptor subunits: diversity, development and disease. Curr Opin Neurobiol 11:327–335

Ehrlich I, Malinow R (2004) Postsynaptic density 95 controls AMPA receptor incorporation during long-term potentiation and experience-driven synaptic plasticity. J Neurosci 24:916–927

Fritschy JM, Weinmann O, Wenzel A, Benke D (1998) Synapse-specific localization of NMDA and GABA(A) receptor subunits revealed by antigen-retrieval immunohistochemistry. J Comp Neurol 390:194–210

Fukaya M, Watanabe M (2000) Improved immunohistochemical detection of postsynaptically located PSD-95/SAP90 protein family by protease section pretreatment: a study in the adult mouse brain. J Comp Neurol 426:572–586

Fukaya M, Tsujita M, Yamazaki M, Kushiya E, Abe M, Akashi K, Natsume R, Kano M, Kamiya H, Watanabe M, Sakimura K (2006) Abundant distribution of TARP gamma-8 in synaptic and extrasynaptic surface of hippocampal neurons and its major role in AMPA receptor expression on spines and dendrites. Eur J Neurosci 24:2177–2190

Fukazawa Y, Shigemoto R (2012) Intra-synapse-type and inter-synapse-type relationships between synaptic size and AMPAR expression. Curr Opin Neurobiol 22:446–452

Gardner SM, Takamiya K, Xia J, Suh JG, Johnson R, Yu S, Huganir RL (2005) Calcium-permeable AMPA receptor plasticity is mediated by subunit-specific interactions with PICK1 and NSF. Neuron 45:903–915

Geiger JR, Melcher T, Koh DS, Sakmann B, Seeburg PH, Jonas P, Monyer H (1995) Relative abundance of subunit mRNAs determines gating and Ca2+ permeability of AMPA receptors in principal neurons and interneurons in rat CNS. Neuron 15:193–204

Greger IH, Khatri L, Ziff EB (2002) RNA editing at arg607 controls AMPA receptor exit from the endoplasmic reticulum. Neuron 34:759–772

Hirai H, Launey T, Mikawa S, Torashima T, Yanagihara D, Kasaura T, Miyamoto A, Yuzaki M (2003) New role of δ2-glutamate receptors in AMPA receptor trafficking and cerebellar function. Nat Neurosci 6:869–876

Huganir RL, Nicoll RA (2013) AMPARs and synaptic plasticity: the last 25 years. Neuron 80:704–717

Isaac JT, Ashby MC, McBain CJ (2007) The role of the GluR2 subunit in AMPA receptor function and synaptic plasticity. Neuron 54:859–871

Jackson AC, Nicoll RA (2011) The expanding social network of ionotropic glutamate receptors: TARPs and other transmembrane auxiliary subunits. Neuron 70:178–199

John HA, Birnstiel ML, Jones KW (1969) RNA–DNA hybrids at the cytological level. Nature 223:582–587

Kashiwabuchi N, Ikeda K, Araki K, Hirano T, Shibuki K, Takayama C, Inoue Y, Kutsuwada T, Yagi T, Kang Y et al (1995) Impairment of motor coordination, Purkinje cell synapse formation, and cerebellar long-term depression in GluR delta 2 mutant mice. Cell 81:245–252

Kawakami R, Shinohara Y, Kato Y, Sugiyama H, Shigemoto R, Ito I (2003) Asymmetrical allocation of NMDA receptor epsilon2 subunits in hippocampal circuitry. Science 300:990–994

Keinanen K, Wisden W, Sommer B, Werner P, Herb A, Verdoorn TA, Sakmann B, Seeburg PH (1990) A family of AMPA-selective glutamate receptors. Science 249:556–560

Kelly L, Farrant M, Cull-Candy SG (2009) Synaptic mGluR activation drives plasticity of calcium-permeable AMPA receptors. Nat Neurosci 12:593–601

Koh DS, Burnashev N, Jonas P (1995a) Block of native Ca(2+)-permeable AMPA receptors in rat brain by intracellular polyamines generates double rectification. J Physiol 486(Pt 2):305–312

Koh DS, Geiger JR, Jonas P, Sakmann B (1995b) Ca(2+)-permeable AMPA and NMDA receptor channels in basket cells of rat hippocampal dentate gyrus. J Physiol 485(Pt 2):383–402

Kullmann DM, Lamsa KP (2007) Long-term synaptic plasticity in hippocampal interneurons. Nat Rev Neurosci 8:687–699

Kurihara H, Hashimoto K, Kano M, Takayama C, Sakimura K, Mishina M, Inoue Y, Watanabe M (1997) Impaired parallel fiber → Purkinje cell synapse stabilization during cerebellar development of mutant mice lacking the glutamate receptor δ2 subunit. J Neurosci 17:9613–9623

Kutsuwada T, Sakimura K, Manabe T, Takayama C, Katakura N, Kushiya E, Natsume R, Watanabe M, Inoue Y, Yagi T, Aizawa S, Arakawa M, Takahashi T, Nakamura Y, Mori H, Mishina M (1996) Impairment of suckling response, trigeminal neuronal pattern formation, and hippocampal LTD in NMDA receptor ε2 subunit mutant mice. Neuron 16:333–344

Lalouette A, Lohof A, Sotelo C, Guenet J, Mariani J (2001) Neurobiological effects of a null mutation depend on genetic context: comparison between two hotfoot alleles of the delta-2 ionotropic glutamate receptor. Neuroscience 105:443–455

Lambolez B, Audinat E, Bochet P, Crepel F, Rossier J (1992) AMPA receptor subunits expressed by single Purkinje cells. Neuron 9:247–258

Landsend AS, Amiry-Moghaddam M, Matsubara A, Bergersen L, Usami S, Wenthold RJ, Ottersen OP (1997) Differential localization of δ glutamate receptors in the rat cerebellum: coexpression with AMPA receptors in parallel fiber–spine synapses and absence from climbing fiber–spine synapses. J Neurosci 17:834–842

Lisman J (1989) A mechanism for the Hebb and the anti-Hebb processes underlying learning and memory. Proc Natl Acad Sci USA 86:9574–9578

Liu SQ, Cull-Candy SG (2000) Synaptic activity at calcium-permeable AMPA receptors induces a switch in receptor subtype. Nature 405:454–458

Lu W, Shi Y, Jackson AC, Bjorgan K, During MJ, Sprengel R, Seeburg PH, Nicoll RA (2009) Subunit composition of synaptic AMPA receptors revealed by a single-cell genetic approach. Neuron 62:254–268

Malinow R, Malenka RC (2002) AMPA receptor trafficking and synaptic plasticity. Annu Rev Neurosci 25:103–126

Masugi-Tokita M, Tarusawa E, Watanabe M, Molnar E, Fujimoto K, Shigemoto R (2007) Number and density of AMPA receptors in individual synapses in the rat cerebellum as revealed by SDS-digested freeze-fracture replica labeling. J Neurosci 27:2135–2144

Matsuda I, Mishina M (2000) Identification of a juxtamembrane segment of the glutamate receptor δ2 subunit required for the plasma membrane localization. Biochem Biophys Res Commun 275:565–571

Matsuda S, Launey T, Mikawa S, Hirai H (2000) Disruption of AMPA receptor GluR2 clusters following long-term depression induction in cerebellar Purkinje neurons. EMBO J 19:2765–2774

Matsuda K, Miura E, Miyazaki T, Kakegawa W, Emi K, Narumi S, Fukazawa Y, Ito-Ishida A, Kondo T, Shigemoto R, Watanabe M, Yuzaki M (2010) Cbln1 is a ligand for an orphan glutamate receptor δ2, a bidirectional synapse organizer. Science 328:363–368

McBain CJ, Dingledine R (1993) Heterogeneity of synaptic glutamate receptors on CA3 stratum radiatum interneurones of rat hippocampus. J Physiol 462:373–392

Misra C, Brickley SG, Farrant M, Cull-Candy SG (2000a) Identification of subunits contributing to synaptic and extrasynaptic NMDA receptors in Golgi cells of the rat cerebellum. J Physiol 524(Pt 1):147–162

Misra C, Brickley SG, Wyllie DJ, Cull-Candy SG (2000b) Slow deactivation kinetics of NMDA receptors containing NR1 and NR2D subunits in rat cerebellar Purkinje cells. J Physiol 525(Pt 2):299–305

Miyazaki T, Fukaya M, Shimizu H, Watanabe M (2003) Subtype switching of vesicular glutamate transporters at parallel fibre-Purkinje cell synapses in developing mouse cerebellum. Eur J Neurosci 17:2563–2572

Momiyama A, Silver RA, Hausser M, Notomi T, Wu Y, Shigemoto R, Cull-Candy SG (2003) The density of AMPA receptors activated by a transmitter quantum at the climbing fibre-Purkinje cell synapse in immature rats. J Physiol 549:75–92

Monyer H, Seeburg PH, Wisden W (1991) Glutamate-operated channels: developmentally early and mature forms arise by alternative splicing. Neuron 6:799–810

Monyer H, Burnashev N, Laurie DJ, Sakmann B, Seeburg PH (1994) Developmental and regional expression in the rat brain and functional properties of four NMDA receptors. Neuron 12:529–540

Mori H, Mishina M (1995) Structure and function of the NMDA receptor channel. Neuropharmacology 34:1219–1237

Nakanishi S, Masu M (1994) Molecular diversity and functions of glutamate receptors. Annu Rev Biophys Biomol Struct 23:319–348

Nicholson DA, Trana R, Katz Y, Kath WL, Spruston N, Geinisman Y (2006) Distance-dependent differences in synapse number and AMPA receptor expression in hippocampal CA1 pyramidal neurons. Neuron 50:431–442

Nimchinsky EA, Yasuda R, Oertner TG, Svoboda K (2004) The number of glutamate receptors opened by synaptic stimulation in single hippocampal spines. J Neurosci 24:2054–2064

Noguchi J, Matsuzaki M, Ellis-Davies GC, Kasai H (2005) Spine–neck geometry determines NMDA receptor-dependent Ca2+ signaling in dendrites. Neuron 46:609–622

Nusser Z, Cull-Candy S, Farrant M (1997) Differences in synaptic GABA(A) receptor number underlie variation in GABA mini amplitude. Neuron 19:697–709

Nusser Z, Lujan R, Laube G, Roberts JD, Molnar E, Somogyi P (1998) Cell type and pathway dependence of synaptic AMPA

receptor number and variability in the hippocampus. Neuron 21:545–559
Nyiri G, Stephenson FA, Freund TF, Somogyi P (2003) Large variability in synaptic N-methyl-D-aspartate receptor density on interneurons and a comparison with pyramidal-cell spines in the rat hippocampus. Neuroscience 119:347–363
Ottersen OP, Landsend AS (1997) Organization of glutamate receptors at the synapse. Eur J Neurosci 9:2219–2224
Palay S, Chan-Palay V (1974) Cerebellar cortex: cytology and organization. Springer, New York
Pellegrini-Giampietro DE, Bennett MV, Zukin RS (1991) Differential expression of three glutamate receptor genes in developing rat brain: an in situ hybridization study. Proc Natl Acad Sci USA 88:4157–4161
Petralia RS, Wenthold RJ (1999) Immunocytochemistry of NMDA receptors. In: Li M(ed) Methods in molecular biology: NMDA receptor protocols. Humana, Totowa, NJ, pp 73–92
Petralia RS, Wang YX, Mayat E, Wenthold RJ (1997) Glutamate receptor subunit 2-selective antibody shows a differential distribution of calcium-impermeable AMPA receptors among populations of neurons. J Comp Neurol 385:456–476
Racca C, Stephenson FA, Streit P, Roberts JD, Somogyi P (2000) NMDA receptor content of synapses in stratum radiatum of the hippocampal CA1 area. J Neurosci 20:2512–2522
Rubio ME, Wenthold RJ (1997) Glutamate receptors are selectively targeted to postsynaptic sites in neurons. Neuron 18:939–950
Sans N, Vissel B, Petralia RS, Wang YX, Chang K, Royle GA, Wang CY, O'Gorman S, Heinemann SF, Wenthold RJ (2003) Aberrant formation of glutamate receptor complexes in hippocampal neurons of mice lacking the GluR2 AMPA receptor subunit. J Neurosci 23:9367–9373
Sato K, Kiyama H, Tohyama M (1993) The differential expression patterns of messenger RNAs encoding non-N-methyl-D-aspartate glutamate receptor subunits (GluR1–4) in the rat brain. Neuroscience 52:515–539
Schnell E, Sizemore M, Karimzadegan S, Chen L, Bredt DS, Nicoll RA (2002) Direct interactions between PSD-95 and stargazin control synaptic AMPA receptor number. Proc Natl Acad Sci USA 99:13902–13907
Seeburg PH (1993) The TINS/TiPS Lecture. The molecular biology of mammalian glutamate receptor channels. Trends Neurosci 16:359–365
Sobczyk A, Scheuss V, Svoboda K (2005) NMDA receptor subunit-dependent [Ca2 +] signaling in individual hippocampal dendritic spines. J Neurosci 25:6037–6046
Stein V, House DR, Bredt DS, Nicoll RA (2003) Postsynaptic density-95 mimics and occludes hippocampal long-term potentiation and enhances long-term depression. J Neurosci 23:5503–5506
Takayama C, Nakagawa S, Watanabe M, Mishina M, Inoue Y (1996) Developmental changes in expression and distribution of the glutamate receptor channel δ2 subunit according to the Purkinje cell maturation. Brain Res Dev Brain Res 92:147–155
Takeuchi T, Miyazaki T, Watanabe M, Mori H, Sakimura K, Mishina M (2005) Control of synaptic connection by glutamate receptor delta2 in the adult cerebellum. J Neurosci 25:2146–2156
Takumi Y, Ramirez-Leon V, Laake P, Rinvik E, Ottersen OP (1999) Different modes of expression of AMPA and NMDA receptors in hippocampal synapses. Nat Neurosci 2:618–624
Tempia F, Kano M, Schneggenburger R, Schirra C, Garaschuk O, Plant T, Konnerth A (1996) Fractional calcium current through neuronal AMPA-receptor channels with a low calcium permeability. J Neurosci 16:456–466
Toth K, McBain CJ (1998) Afferent-specific innervation of two distinct AMPA receptor subtypes on single hippocampal interneurons. Nat Neurosci 1:572–578
Tsuzuki K, Lambolez B, Rossier J, Ozawa S (2001) Absolute quantification of AMPA receptor subunit mRNAs in single hippocampal neurons. J Neurochem 77:1650–1659
Uemura T, Kakizawa S, Yamasaki M, Sakimura K, Watanabe M, Iino M, Mishina M (2007) Regulation of long-term depression and climbing fiber territory by glutamate receptor δ2 at parallel fiber synapses through its C-terminal domain in cerebellar Purkinje cells. J Neurosci 27:12096–12108
Wang YT, Linden DJ (2000) Expression of cerebellar long-term depression requires postsynaptic clathrin-mediated endocytosis. Neuron 25:635–647
Watanabe M, Inoue Y, Sakimura K, Mishina M (1992) Developmental changes in distribution of NMDA receptor channel subunit mRNAs. NeuroReport 3:1138–1140
Watanabe M, Fukaya M, Sakimura K, Manabe T, Mishina M, Inoue Y (1998) Selective scarcity of NMDA receptor channel subunits in the stratum lucidum (mossy fibre-recipient layer) of the mouse hippocampal CA3 subfield. Eur J Neurosci 10:478–487
Wenthold RJ, Petralia RS, Blahos J II, Niedzielski AS (1996) Evidence for multiple AMPA receptor complexes in hippocampal CA1/CA2 neurons. J Neurosci 16:1982–1989
Yamasaki M, Miyazaki T, Azechi H, Abe M, Natsume R, Hagiwara T, Aiba A, Mishina M, Sakimura K, Watanabe M (2011) Glutamate receptor δ2 is essential for input pathway-dependent regulation of synaptic AMPAR contents in cerebellar Purkinje cells. J Neurosci 31:3362–3374
Yamasaki M, Okada R, Takasaki C, Toki S, Fukaya M, Natsume R, Sakimura K, Mishina M, Shirakawa T, Watanabe M (2014) Opposing role of NMDA receptor GluN2B and GluN2D in somatosensory development and maturation. J Neurosci 34:11534–11548
Yuzaki M (2009) New (but old) molecules regulating synapse integrity and plasticity: Cbln1 and the δ2 glutamate receptor. Neuroscience 162:633–643
Ziff EB (2007) TARPs and the AMPA receptor trafficking paradox. Neuron 53:627–633